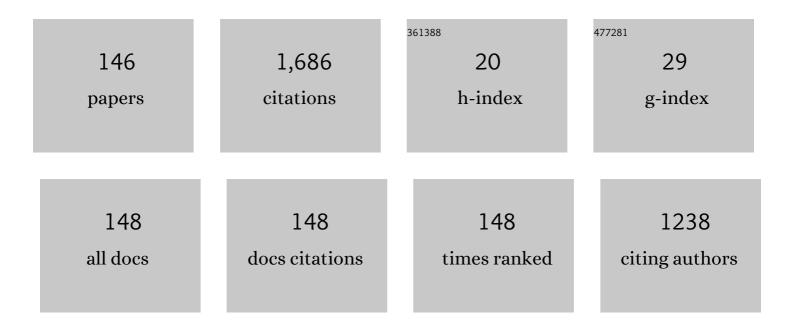
Luc Stafford

List of Publications by Year in descending order

Source: https://exaly.com/author-pdf/7490770/publications.pdf Version: 2024-02-01



#	Article	IF	CITATIONS
1	Deposition of Hydrophobic Functional Groups on Wood Surfaces Using Atmosphericâ€Pressure Dielectric Barrier Discharge in Heliumâ€Hexamethyldisiloxane Gas Mixtures. Plasma Processes and Polymers, 2012, 9, 1168-1175.	3.0	71
2	Modification of Sugar Maple (Acer saccharum) and Black Spruce (Picea mariana) Wood Surfaces in a Dielectric Barrier Discharge (DBD) at Atmospheric Pressure. Journal of Adhesion Science and Technology, 2010, 24, 1401-1413.	2.6	53
3	Improved water repellency of black spruce wood surfaces after treatment in carbon tetrafluoride plasmas. Wood Science and Technology, 2013, 47, 411-422.	3.2	44
4	Deposition of nanocomposite coatings on wood using cold discharges at atmospheric pressure. Surface and Coatings Technology, 2017, 309, 729-737.	4.8	43
5	Development of Organosilicon-Based Superhydrophobic Coatings through Atmospheric Pressure Plasma Polymerization of HMDSO in Nitrogen Plasma. Materials, 2019, 12, 219.	2.9	42
6	Role of substrate outgassing on the formation dynamics of either hydrophilic or hydrophobic wood surfaces in atmospheric-pressure, organosilicon plasmas. Surface and Coatings Technology, 2013, 234, 42-47.	4.8	34
7	Recombination of chlorine atoms on plasma-conditioned stainless steel surfaces in the presence of adsorbed Cl ₂ . Journal Physics D: Applied Physics, 2009, 42, 055206.	2.8	33
8	Nebulization of Nanocolloidal Suspensions for the Growth of Nanocomposite Coatings in Dielectric Barrier Discharges. Plasma Processes and Polymers, 2016, 13, 981-989.	3.0	33
9	Preferential self-healing at grain boundaries in plasma-treated graphene. Nature Materials, 2021, 20, 49-54.	27.5	31
10	Energy dependence of ion-assisted chemical etch rates in reactive plasmas. Applied Physics Letters, 2005, 87, 071502.	3.3	28
11	Critical review: Plasma-surface reactions and the spinning wall method. Journal of Vacuum Science and Technology A: Vacuum, Surfaces and Films, 2011, 29, .	2.1	28
12	Determination of active species in the modification of hardwood samples in the flowing afterglow of N2 dielectric barrier discharges open to ambient air. Cellulose, 2015, 22, 811-827.	4.9	27
13	Influence of the voltage waveform during nanocomposite layer deposition by aerosol-assisted atmospheric pressure Townsend discharge. Journal of Applied Physics, 2016, 120, .	2.5	27
14	Effects of Zn content on structural and transparent conducting properties of indium-zinc oxide films grown by rf magnetron sputtering. Journal of Vacuum Science & Technology B, 2006, 24, 2737.	1.3	25
15	Recombination probability of oxygen atoms on dynamic stainless steel surfaces in inductively coupled O2 plasmas. Journal of Vacuum Science and Technology A: Vacuum, Surfaces and Films, 2008, 26, 455-461.	2.1	24
16	Electron density and temperature in an atmospheric-pressure helium diffuse dielectric barrier discharge from kHz to MHz. Plasma Sources Science and Technology, 2018, 27, 035005.	3.1	24
17	In-Situ Surface Recombination Measurements of Oxygen Atoms on Anodized Aluminum in an Oxygen Plasma. Journal of Physical Chemistry C, 2008, 112, 8963-8968.	3.1	23
18	Effect of Wood Surface Modification by Atmospheric-Pressure Plasma on Waterborne Coating Adhesion. BioResources, 2014, 9, .	1.0	23

#	Article	IF	CITATIONS
19	Spectroscopic diagnostics of low-pressure inductively coupled Kr plasma using a collisional–radiative model with fully relativistic cross sections. Plasma Sources Science and Technology, 2016, 25, 035025.	3.1	21
20	Interaction of atomized colloid with an ac electric field in a dielectric barrier discharge reactor used for deposition of nanocomposite coatings. Journal Physics D: Applied Physics, 2017, 50, 075201.	2.8	21
21	Characterization of a microwave argon plasma column at atmospheric pressure by optical emission and absorption spectroscopy coupled with collisional-radiative modelling. Physics of Plasmas, 2019, 26, 063516.	1.9	21
22	Schottky barrier height of boride-based rectifying contacts to p-GaN. Applied Physics Letters, 2006, 89, 132110.	3.3	20
23	Determination of the electron temperature in plane-to-plane He dielectric barrier discharges at atmospheric pressure. Plasma Sources Science and Technology, 2016, 25, 015011.	3.1	20
24	Kinetics driving high-density chlorine plasmas. Journal of Applied Physics, 2005, 98, 063301.	2.5	19
25	Toward More Sustainable Rechargeable Aqueous Batteries Using Plasma-Treated Cellulose-Based Li-Ion Electrodes. ACS Sustainable Chemistry and Engineering, 2020, 8, 4728-4733.	6.7	19
26	Influence of redeposition on the plasma etching dynamics. Journal of Applied Physics, 2007, 101, 083303.	2.5	18
27	Optical emission spectroscopy of microwave-plasmas at atmospheric pressure applied to the growth of organosilicon and organotitanium nanopowders. Journal of Applied Physics, 2014, 115, .	2.5	18
28	Cyclic evolution of the electron temperature and density in dusty low-pressure radio frequency plasmas with pulsed injection of hexamethyldisiloxane. Applied Physics Letters, 2015, 107, .	3.3	18
29	Modification of hardwood samples in the flowing afterglow of N2–O2 dielectric barrier discharges open to ambient air. Cellulose, 2015, 22, 3397-3408.	4.9	18
30	On the Icephobic Behavior of Organosilicon-Based Surface Structures Developed Through Atmospheric Pressure Plasma Deposition in Nitrogen Plasma. Coatings, 2019, 9, 679.	2.6	18
31	Low-damage nitrogen incorporation in graphene films by nitrogen plasma treatment: Effect of airborne contaminants. Carbon, 2019, 144, 532-539.	10.3	18
32	Sputter-etching characteristics of barium–strontium–titanate and bismuth–strontium–tantalate using a surface-wave high-density plasma reactor. Journal of Vacuum Science and Technology A: Vacuum, Surfaces and Films, 2002, 20, 530-535.	2.1	17
33	Niâ^•Au Ohmic contacts to p-type Mg-doped CuCrO2 epitaxial layers. Applied Physics Letters, 2007, 90, 142101.	3.3	17
34	Ohmic contacts to p-type GaN based on TaN, TiN, and ZrN. Applied Physics Letters, 2007, 90, 212107.	3.3	17
35	Effect of cryogenic temperature deposition on Au contacts to bulk, single-crystal n-type ZnO. Applied Surface Science, 2007, 253, 3766-3772.	6.1	17
36	Effect of Cu contamination on recombination of O atoms on a plasma-oxidized silicon surface. Journal of Applied Physics, 2009, 105, .	2.5	17

#	Article	IF	CITATIONS
37	Experimental and modeling study of O and Cl atoms surface recombination reactions in O2 and Cl2 plasmas. Pure and Applied Chemistry, 2010, 82, 1301-1315.	1.9	17
38	Electrical characterization of the flowing afterglow of N2 and N2/O2 microwave plasmas at reduced pressure. Journal of Applied Physics, 2014, 115, .	2.5	17
39	Improved long-term thermal stability of InGaNâ^•GaN multiple quantum well light-emitting diodes using TiB2- and Ir-based p-Ohmic contacts. Applied Physics Letters, 2007, 90, 242103.	3.3	16
40	Dry etching of zinc-oxide and indium-zinc-oxide in IBr and BI3 plasma chemistries. Applied Surface Science, 2007, 253, 3773-3778.	6.1	16
41	Surface free radicals detection using molecular scavenging method on black spruce wood treated with cold, atmospheric-pressure plasmas. Applied Surface Science, 2015, 359, 137-142.	6.1	16
42	Time-resolved study of the electron temperature and number density of argon metastable atoms in argon-based dielectric barrier discharges. Plasma Sources Science and Technology, 2018, 27, 015015.	3.1	16
43	Influence of N ₂ , O ₂ , and H ₂ admixtures on the electron power balance and neutral gas heating in microwave Ar plasmas at atmospheric pressure. Journal Physics D: Applied Physics, 2019, 52, 475201.	2.8	16
44	Recent progress on organosilicon coatings deposited on bleached unrefined Kraft paper by non-thermal plasma process at atmospheric pressure. Progress in Organic Coatings, 2020, 147, 105865.	3.9	16
45	Analysis of transport phenomena during plasma deposition of hydrophobic coatings on porous cellulosic substrates in planeâ€toâ€plane dielectric barrier discharges at atmospheric pressure. Plasma Processes and Polymers, 2020, 17, 2000091.	3.0	16
46	Barium–strontium–titanate etching characteristics in chlorinated discharges. Journal of Vacuum Science and Technology A: Vacuum, Surfaces and Films, 2003, 21, 1247-1252.	2.1	15
47	Microfabricated SrTiO3 ridge waveguides. Applied Physics Letters, 2005, 86, 221106.	3.3	15
48	Influence of substrate outgassing on the plasma properties during wood treatment in He dielectric barrier discharges at atmospheric pressure. Plasma Processes and Polymers, 2017, 14, 1600172.	3.0	15
49	Multi-scale investigation in the frequency domain of Ar/HMDSO dusty plasma with pulsed injection of HMDSO. Plasma Sources Science and Technology, 2019, 28, 055019.	3.1	15
50	Deposition of fluorocarbon groups on wood surfaces using the jet of an atmospheric-pressure dielectric barrier discharge. Wood Science and Technology, 2017, 51, 1339-1352.	3.2	14
51	Characterization of neutral, positive, and negative species in a chlorine high-density surface-wave plasma. Journal of Applied Physics, 2003, 93, 1907-1913.	2.5	13
52	High-density plasma etching of indium–zinc oxide films in Ar/Cl2 and Ar/CH4/H2 chemistries. Applied Surface Science, 2006, 253, 2752-2757.	6.1	13
53	Electron energy distribution functions in low-pressure oxygen plasma columns sustained by propagating surface waves. Applied Physics Letters, 2009, 94, 021503.	3.3	13
54	Populations of metastable and resonant argon atoms in radio frequency magnetron plasmas used for deposition of indium-zinc-oxide films. Journal of Vacuum Science and Technology A: Vacuum, Surfaces and Films, 2012, 30, .	2.1	13

#	Article	IF	CITATIONS
55	Time-resolved imaging of pulsed positive nanosecond discharge on water surface: plasma dots guided by water surface. Plasma Sources Science and Technology, 2020, 29, 115017.	3.1	13
56	A combination of plasma diagnostics and Raman spectroscopy to examine plasma-graphene interactions in low-pressure argon radiofrequency plasmas. Journal of Applied Physics, 2019, 126, .	2.5	12
57	TiO ₂ –SiO ₂ nanocomposite thin films deposited by direct liquid injection of colloidal solution in an O ₂ /HMDSO low-pressure plasma. Journal Physics D: Applied Physics, 2021, 54, 085206.	2.8	12
58	On the validity of neutral gas temperature by N ₂ rovibrational spectroscopy in low-pressure inductively coupled plasmas. Plasma Sources Science and Technology, 2011, 20, 035016.	3.1	11
59	Experimental and modelling study of organization phenomena in dielectric barrier discharges with structurally inhomogeneous wood substrates. Plasma Sources Science and Technology, 2014, 23, 054006.	3.1	11
60	Characterization of argon dielectric barrier discharges applied to ethyl lactate plasma polymerization. Journal Physics D: Applied Physics, 2017, 50, 475205.	2.8	11
61	Treatment of graphene films in the early and late afterglows of N ₂ plasmas: comparison of the defect generation and N-incorporation dynamics. Plasma Sources Science and Technology, 2018, 27, 124004.	3.1	11
62	Multi-pass deposition of organosilicon-based superhydrophobic coatings in atmospheric pressure plasma jets. Thin Solid Films, 2020, 714, 138369.	1.8	11
63	Deposition of antiâ€fog coatings on glass substrates using the jet of an openâ€ŧoâ€air microwave argon plasma at atmospheric pressure. Plasma Processes and Polymers, 2020, 17, 1900229.	3.0	11
64	Unveiling the origin of the anti-fogging performance of plasma-coated glass: Role of the structure and the chemistry of siloxane precursors. Progress in Organic Coatings, 2020, 141, 105401.	3.9	10
65	Modification of microfibrillated cellulosic foams in a dielectric barrier discharge at atmospheric pressure. Plasma Processes and Polymers, 2021, 18, 2000158.	3.0	10
66	Dependence of the sputter-etching characteristics of strontium–titanate–oxide thin films on their structural properties. Applied Physics Letters, 2004, 84, 2500-2502.	3.3	9
67	Influence of the Microstructure on the Optical Characteristics of SrTiO3 thin films. Journal of Materials Research, 2005, 20, 68-74.	2.6	9
68	Influence of ion mixing on the energy dependence of the ion-assisted chemical etch rate in reactive plasmas. Journal of Applied Physics, 2006, 100, 063309.	2.5	9
69	Increased Schottky barrier heights for Au on n- and p-type GaN using cryogenic metal deposition. Applied Physics Letters, 2006, 89, 122106.	3.3	9
70	Influence of the film properties on the plasma etching dynamics of rf-sputtered indium zinc oxide layers. Journal of Vacuum Science and Technology A: Vacuum, Surfaces and Films, 2007, 25, 659-665.	2.1	9
71	W 2 B and CrB2 diffusion barriers for Niâ^•Au contacts to p-GaN. Applied Physics Letters, 2007, 91, .	3.3	9
72	Simulation of redeposition during platinum etching in argon plasmas. Journal of Applied Physics, 2010, 107, 063306.	2.5	9

#	Article	IF	CITATIONS
73	Nonlocal effect of plasma resonances on the electron energy-distribution function in microwave plasma columns. Physical Review E, 2012, 86, 015402.	2.1	9
74	Improvement of the emission properties from InGaN/GaN dot-in-a-wire nanostructures after treatment in the flowing afterglow of a microwave N ₂ plasma. Nanotechnology, 2014, 25, 435606.	2.6	9
75	Enhancing the water repellency of wood surfaces by atmospheric pressure cold plasma deposition of fluorocarbon film. RSC Advances, 2017, 7, 29159-29169.	3.6	9
76	Timeâ€resolved analysis of the precursor fragmentation kinetics in an hybrid PVD/PECVD dusty plasma with pulsed injection of HMDSO. Plasma Processes and Polymers, 2019, 16, 1900044.	3.0	9
77	Modification of the optical properties and nano-crystallinity of anatase TiO2nanoparticles thin film using low pressure O2 plasma treatment. Thin Solid Films, 2020, 709, 138212.	1.8	9
78	Probing plasma-treated graphene using hyperspectral Raman. Review of Scientific Instruments, 2020, 91, 063903.	1.3	9
79	Response surface methodology as a predictive tool for the fabrication of coatings with optimal anti-fogging performance. Thin Solid Films, 2021, 718, 138482.	1.8	9
80	Effect of extractives in plasma modification of wood surfaces. Surface Innovations, 2015, 3, 196-205.	2.3	8
81	Selective nitrogen doping of graphene due to preferential healing of plasma-generated defects near grain boundaries. Npj 2D Materials and Applications, 2020, 4, .	7.9	8
82	lon mass dependence of the etch yield of SrTiO3 films in reactive plasmas. Applied Physics Letters, 2005, 87, 131503.	3.3	7
83	Thermal stability of Ohmic contacts to InN. Applied Physics Letters, 2007, 90, 162107.	3.3	7
84	Comparison of plasma chemistries for the dry etching of bulk single-crystal zinc-oxide and rf-sputtered indium–zinc-oxide films. Applied Surface Science, 2007, 253, 9228-9233.	6.1	7
85	Annealing and Measurement Temperature Dependence of W2B- and W2B5-Based Rectifying Contacts to p-GaN. Journal of Electronic Materials, 2007, 36, 384-390.	2.2	7
86	Aging and Stability of GaN High Electron Mobility Transistors and Light-Emitting Diodes With \$hbox{TiB}_{2}\$- and Ir-Based Contacts. IEEE Transactions on Device and Materials Reliability, 2008, 8, 272-276.	2.0	7
87	Emission spectra from direct current and microwave powered Hg lamps at very high pressure. Journal Physics D: Applied Physics, 2013, 46, 455201.	2.8	7
88	Beyond microelectronics with 1,3,5,7-tetramethylcyclotetrasiloxane: A promising molecule for anti-fogging coatings. Materials Chemistry and Physics, 2020, 242, 122508.	4.0	7
89	Spatially-Resolved Spectroscopic Diagnostics of a Miniature RF Atmospheric Pressure Plasma Jet in Argon Open to Ambient Air. Plasma, 2020, 3, 38-53.	1.8	7
90	Influence of the positive ion composition on the ion-assisted chemical etch yield of SrTiO3 films in Arâ^•SF6 plasmas. Journal of Vacuum Science and Technology A: Vacuum, Surfaces and Films, 2007, 25, 425-431.	2.1	6

#	Article	IF	CITATIONS
91	Ir-based diffusion barriers for Ohmic contacts to p-GaN. Applied Surface Science, 2008, 254, 4134-4138.	6.1	6
92	Measurements of sputtered neutrals and ions and investigation of their roles on the plasma properties during rf magnetron sputtering of Zn and ZnO targets. Journal of Vacuum Science and Technology A: Vacuum, Surfaces and Films, 2013, 31, 061306.	2.1	6
93	Microstructural and optical properties tuning of BiFeO3 thin films elaborated by magnetron sputtering. Journal of Materials Science: Materials in Electronics, 2015, 26, 3316-3323.	2.2	6
94	Correlation between surface chemistry and ion energy dependence of the etch yield in multicomponent oxides etching. Journal of Applied Physics, 2009, 106, .	2.5	5
95	Characterization of a low-pressure chlorine plasma column sustained by propagating surface waves using phase-sensitive microwave interferometry and trace-rare-gas optical emission spectroscopy. Journal of Applied Physics, 2011, 109, 113304.	2.5	5
96	Evidence of local power deposition and electron heating by a standing electromagnetic wave in electron-cyclotron-resonance plasma. Physical Review E, 2014, 90, 033106.	2.1	5
97	Organization of Dielectric Barrier Discharges in the Presence of Structurally Inhomogeneous Wood Substrates. IEEE Transactions on Plasma Science, 2014, 42, 2366-2367.	1.3	5
98	Highly porous micro-roughened structures developed on aluminum surface using the jet of rotating arc discharges at atmospheric pressure. Journal of Applied Physics, 2018, 123, .	2.5	5
99	Influence of a square pulse voltage on argon-ethyl lactate discharges and their plasma-deposited coatings using time-resolved spectroscopy and surface characterization. Physics of Plasmas, 2018, 25, 103504.	1.9	5
100	Analysis of the high-energy electron population in surface-wave plasma columns in presence of collisionless resonant absorption. Plasma Sources Science and Technology, 2018, 27, 095011.	3.1	5
101	Emission and absorption diagnostics of a diffuse dielectric barrier discharge with multiple current peaks in helium at atmospheric pressure. Plasma Sources Science and Technology, 2019, 28, 085011.	3.1	5
102	Experiments and kinetic modeling of the ion energy distribution function at the substrate surface during magnetron sputtering of silver targets in radio frequency argon plasmas. Journal of Vacuum Science and Technology A: Vacuum, Surfaces and Films, 2019, 37, 021301.	2.1	5
103	Refined analysis of current–voltage characteristics in Townsend dielectric barrier discharges in nitrogen at atmospheric pressure. Journal Physics D: Applied Physics, 2021, 54, 095204.	2.8	5
104	Role of excimer formation and induced photoemission on the Ar metastable kinetics in atmospheric pressure Ar–NH ₃ dielectric barrier discharges. Plasma Sources Science and Technology, 2022, 31, 065010.	3.1	5
105	Propagation of surface waves in two-plasma systems bounded by a metallic enclosure. Journal of Plasma Physics, 2001, 66, 349-362.	2.1	4
106	Ir-Based Schottky and Ohmic Contacts on n-GaN. Journal of the Electrochemical Society, 2007, 154, H584.	2.9	4
107	Nanoparticle synthesis by high-density plasma sustained in liquid organosilicon precursors. Journal of Applied Physics, 2017, 122, .	2.5	4
108	Atmospheric pressure Townsend discharges as a promising tool for the oneâ€step deposition of antifogging coatings from N 2 O/TMCTS mixtures. Plasma Processes and Polymers, 2020, 17, 1900186.	3.0	4

#	Article	IF	CITATIONS
109	On the rotational–translational equilibrium in non-thermal argon plasmas at atmospheric pressure. Plasma Sources Science and Technology, 2021, 30, 035020.	3.1	4
110	Comment on "Plasma etching of high dielectric constant materials on silicon in halogen plasma chemistries―by L. Sha and J. P. Chang [J. Vac. Sci. Technol. A 22, 88 (2004)]. Journal of Vacuum Science and Technology A: Vacuum, Surfaces and Films, 2005, 23, 720-721.	2.1	3
111	Effect of Cryogenic Temperature Deposition of Various Metal Contacts on Bulk Single-Crystal n-Type ZnO. Journal of Electronic Materials, 2007, 36, 488-493.	2.2	3
112	Determination of the number density of excited and ground Zn atoms during rf magnetron sputtering of ZnO target. Journal of Vacuum Science and Technology A: Vacuum, Surfaces and Films, 2015, 33, 041302.	2.1	3
113	Probing suprathermal electrons by trace rare gases optical emission spectroscopy in low pressure dipolar microwave plasmas excited at the electron cyclotron resonance. Physics of Plasmas, 2018, 25, .	1.9	3
114	Time and space-resolved experimental investigation of the electron energy distribution function of a helium capacitive discharge at atmospheric pressure. Journal Physics D: Applied Physics, 2019, 52, 245202.	2.8	3
115	Ultra-high-resolution optical absorption spectroscopy of DC plasmas at low pressure using a supercontinuum laser combined with a laser line tunable filter and a HyperFine spectrometer. Journal Physics D: Applied Physics, 2021, 54, 085204.	2.8	3
116	Growth and patterning of strontium-titanate-oxide thin films for optical devices applications. Materials Research Society Symposia Proceedings, 2004, 817, 141.	0.1	2
117	Irâ^•Au Ohmic Contacts on Bulk, Single-Crystal n-Type ZnO. Journal of the Electrochemical Society, 2007, 154, H161.	2.9	2
118	Nitride-based Ohmic and Schottky Contacts to GaN. ECS Transactions, 2007, 6, 191-199.	0.5	2
119	Deep etch-induced damage during ion-assisted chemical etching of sputtered indium–zinc–oxide films in Ar/CH4/H2 plasmas. Thin Solid Films, 2008, 516, 2869-2873.	1.8	2
120	Spatially Modulated Emission of ECR Plasmas in Helium. IEEE Transactions on Plasma Science, 2014, 42, 2762-2763.	1.3	2
121	Spatially resolved electron density and electron energy distribution function in Ar magnetron plasmas used for sputter-deposition of ZnO-based thin films. Journal of Vacuum Science and Technology A: Vacuum, Surfaces and Films, 2015, 33, 061310.	2.1	2
122	In situ investigation of magnetron sputtering plasma used for the deposition of multiferroic BiFeO3 thin films. Journal of Materials Science: Materials in Electronics, 2017, 28, 15749-15753.	2.2	2
123	Interaction of N and O atoms with hardwood and softwood surfaces in the flowing afterglow of N ₂ â€O ₂ microwave plasmas. Plasma Processes and Polymers, 2018, 15, e1800035.	3.0	2
124	Plasma–graphene interactions: combined effects of positive ions, vacuum-ultraviolet photons, and metastable species. Journal Physics D: Applied Physics, 2021, 54, 295202.	2.8	2
125	Characterization of non-thermal dielectric barrier discharges at atmospheric pressure in presence of microfibrillated cellulosic foams. Plasma Sources Science and Technology, 2021, 30, 095019.	3.1	2
126	Spatio-temporal dynamics of a nanosecond pulsed microwave plasma ignited by time reversal. Plasma Sources Science and Technology, 2020, 29, 125017.	3.1	2

#	Article	IF	CITATIONS
127	Reduction of Dry Etch Damage to GaAs Using Pulse-Time Modulated Plasmas. Electrochemical and Solid-State Letters, 2007, 10, H139.	2.2	1
128	Thermally Stable Novel Metal Contacts on Bulk, Single-Crystal n-type ZnO. ECS Transactions, 2007, 6, 279-284.	0.5	1
129	Improved Long-Term Thermal Stability At 350°C Of TiB2–Based Ohmic Contacts On AlGaN/GaN High Electron Mobility Transistors. Journal of Electronic Materials, 2007, 36, 379-383.	2.2	1
130	Thermal Stability of Nitride-Based Diffusion Barriers for Ohmic Contacts to n-GaN. Journal of Electronic Materials, 2007, 36, 1662-1668.	2.2	1
131	Deposition of TiO ₂ -SiO ₂ nanocomposite coatings using atmospheric-pressure plasmas. , 2016, , .		1
132	Parametric study of the electron temperature and density in dusty low-pressure RF plasmas with pulsed injection of hexamethyldisiloxane. , 2016, , .		1
133	Incorporation-limiting mechanisms during nitrogenation of monolayer graphene films in nitrogen flowing afterglows. Nanoscale, 2021, 13, 2891-2901.	5.6	1
134	Growth, Characterization and Processing of VO2 Thin Films for Micro-switching Devices. Materials Research Society Symposia Proceedings, 2005, 872, 1.	0.1	0
135	GaN-Based Devices for Reliable Operation at Very High Temperatures. ECS Transactions, 2006, 3, 349-357.	0.5	0
136	Effect of Cryogenic Temperature Deposition of Various Metal Contacts to Bulk, Single-Crystal n-type ZnO. Materials Research Society Symposia Proceedings, 2006, 957, 1.	0.1	0
137	Novel Thermally Stable Contacts to GaN. ECS Transactions, 2006, 3, 341-347.	0.5	0
138	Ir/Au Ohmic Contacts on Bulk, Single-Crystal n-Type ZnO. Materials Research Society Symposia Proceedings, 2007, 1000, 1.	0.1	0
139	High Density Inductively Coupled Plasma Etching of Zinc-Oxide(ZnO) and Indium-Zinc Oxide(IZO). ECS Transactions, 2007, 6, 239-247.	0.5	0
140	High temperature Ohmic contacts to p-type GaN for use in light emitting applications. Physica Status Solidi C: Current Topics in Solid State Physics, 2008, 5, 2241-2243.	0.8	0
141	In-situ Surface Recombination Measurement of Oxygen and Chlorine Atoms on Dynamic Stainless Steel Surfaces in Inductively Coupled O2 and Cl2 Plasmas. ECS Transactions, 2008, 13, 23-32.	0.5	0
142	High Temperature Stable Contacts for GaN HEMTs and LEDs. Materials Research Society Symposia Proceedings, 2008, 1108, 1.	0.1	0
143	Collisional-radiative model for the diagnostics of low pressure inductively coupled krypton plasma. , 2014, , .		0
144	Experimental study of nanoparticle formation dynamics in HMDSO-Ar asymmetric capacitively-coupled radiofrequency plasma with application to deposition of nanocomposite layers. , 2016, , .		0

#	Article	IF	CITATIONS
145	Development of a highly porous alumina-based structure on an aluminum surface using APPJ treatment. , 2016, , .		0
146	Postgrowth modification of monolayer graphene films by low-pressure diborane-argon plasma. Journal of Vacuum Science and Technology A: Vacuum, Surfaces and Films, 2021, 39, 043003.	2.1	0